Non-reflecting boundary condition for surface water wave simulation in the vicinity of a solid body

Jose M. Orellana

Monografías Matemáticas *García de Galdeano* **vv**, 1–**??** (yyyy)

NON-REFLECTING BOUNDARY CONDITION FOR SURFACE WATER WAVE SIMULATION IN THE VICINITY OF A SOLID BODY

J. M. Orellana

Abstract. In this paper, we focus on the modelling of the wake of a solid body moving through the water. To this end, the flow of an inviscid, barotropic and compressible fluid around the solid body regarded as motionless is examined. The dynamic behaviour of the fluid is analysed by means of a two-dimensional Neumann-Kelvin's coupled model enhanced with capillarity and inertia terms. For computational purposes, the unbounded spatial domain must be truncated and then suitable absorbing boundary conditions are introduced. Difficulties arise mainly from the important difference between properties of the inner water and the water surface. Singularities appear on the intersection between the boundaries of the domain and the air-fluid interface. Very different dynamical responses are noticed according to the location of excitation with respect to the free surface. Numerical illustrations of these results are given and commented.

Keywords: water waves, non-reflecting boundary condition, fluid-structure interaction, numerical instabilities.

AMS classification: Primary: 74F10, 35L85, 35R35; Secondary: 76B15, 35L70, 35Q35.

§1. Preliminaries

1.1. Introduction

Understanding wave propagation mechanisms on the sea has long been a subject of interest for many researchers [7], [9], [12]. Surface water wave phenomenon is due to the balance between the gravity forces that keep horizontal free surface of the water, the surface tension that keeps the consistency of the air-water interface, the water inertia and the difference between air and water pressure. According to the relevant effect that forces the motion, the waves are usually divided in gravity waves, capillary waves or pressure waves. In our case, the waves are regarded as interfacial gravity-capillary waves propagating between two liquid layers with very different properties. The upper layer is the free surface water with an infinitesimal thickness and small characteristic velocity of wave propagation namely, riddle velocity. The lower layer is the inner water with a finite or semi infinite thickness and an high characteristic velocity of wave propagation namely the speed of sound in water. The waves are generated by the movement of the solid body, interacting with its rigid surface and propagating all around it, leading to a wake in its vicinity. Free surface flow induced by an immersed moving body problem is relevant to numerous pratical applications in hydrodynamics and aerodynamics. Many theoretical models and numerical methods have been

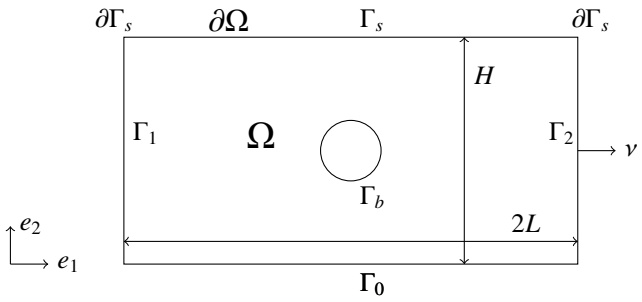

Figure 1: Geometry and notations of the problem.

developed to simulate the body-fluid interaction (cf. [10], [8], [11]). After stating the problem and specifying underlying assumptions, a two dimensional Neumann-Kelvin's coupled modelization enhanced with capillarity and inertia terms is proposed (cf. [3]). A linearization around a steady state is performed and accurate boundary conditions are introduced to carry out the study in an open domain artificially bounded for computational limitation reasons. The variational formulation of the problem is deduced and a finite element approximation in space with a centered finite difference scheme in time is used to approach the solution. Results are illustrated and discussed.

1.2. Problem statement

Our purpose is to determine the dynamical behaviour of the water surface in the vicinity of a solid body that moves with an horizontal velocity U and with a possible oscillatory displacement. To this end, we examine the flow irrotationnal and unviscid of a compressible and barotropic fluid around the structure seen as fixed. Due to the existence of singularities at contact points between surface solid body and surface of water and at underwater angular points, the structure is immersed and its shape is simplified to a cylinder. We consider as computational domain a rectangular open domain $\Omega = [-L, L] \times [0, H]$ with an hole of radius R in its center. Its boundary $\partial\Omega = \Gamma_0 \cup \Gamma_1 \cup \Gamma_s \cup \Gamma_2 \cup \Gamma_b$ has unit outward normal vector ν. Γ_0 correponds to the bottom of the system, Γ_s, to the free surface of the water, Γ_1 and Γ_2, to the sides through which the water flow enters and leaves Ω and Γ_b , to the rigid body surface (see Figure 1). $\partial\Gamma_s$ denotes the edges of Γ_s. For numerical computations, $L = 1\,m, H = 1\,m, R = 5.10^{-2}\,m$, $U = 0.15\,m.s^{-1}$. A steady flow passes through Ω with horizontal velocity U and a small disturbance is introduced inside or on the surface of the fluid.

§2. Theoretical modelling

The propagating medium consists of two liquid layers with very different properties and then two models have to be introduced to take these features into account: an inner fluid model and a surface model. The global nonlinear dynamical model obtained is linearized around a steady state. Therefore the global solution is split into a steady state and a transient one.

The lateral boundary conditions are defined separately according to the nature of the state. For the steady flow, the most realistic condition is to set the normal velocity. For transient flow, non-reflecting boundary conditions (NRBC) have to be prescribed for the inlet and the outlet of Ω in order to avoid any spurious rebounds of the waves reaching the boundaries of the domain.

2.1. Hypotheses and formulation of the global model

2.1.1. Formulation of the inner fluid model

We assume that the flow is characterized by two variables modelling the mass density ρ_{tot} and the velocity potential Φ that satisfy:

- the conservation of mass equation,

$$\frac{\partial \rho_{tot}}{\partial t} + \mathrm{div}(\rho_{tot} \nabla \Phi) = 0 \ \text{ in } \ \Omega \times]0, T[\,, \tag{1}$$

- the Bernoulli equation for unsteady compressible potential flow (neglecting gravity effect),

$$\frac{\partial \Phi}{\partial t} + \frac{1}{2} \|\nabla \Phi\|^2 + F(\rho_{tot}) = 0 \ \text{ in } \ \Omega \times]0, T[\tag{2}$$

where $F(\rho_{tot}) = \int_{\rho_0}^{\rho_{tot}} \frac{1 \partial p}{\rho \partial \rho} d\rho + F(\rho_0)$ is the barotropic potential, p, the fluid pressure and T, the simulation time.

2.1.2. Formulation of the surface model

Applying Newton's second law of motion to a infinitesimal small surface element of thickness 2ε that vertically moves η_{tot}, leads to the free surface equilibrium equation:

$$2\varepsilon \rho_{tot} \frac{D^2 \eta_{tot}}{Dt^2} = -\rho_{tot} \frac{\partial \Phi}{\partial t} - \frac{\rho_{tot}}{2} \|\nabla_s \Phi\|^2 + \sigma \Delta_s \eta_{tot} - \rho_{tot} g \eta_{tot} \quad \text{in} \quad \Gamma_s \times]0, T[\,, \tag{3}$$

where the forces involved consist in the capillary action $\sigma \Delta_s \eta_{tot}$, the gravity force $-\rho_{tot} g \eta_{tot}$ and the pressure $-\rho_{tot} \frac{\partial \Phi}{\partial t} - \frac{\rho_{tot}}{2} \|\nabla_s \Phi\|^2$ (cf. [3]). For water, the surface tension σ is equal to $0.075 N.m^{-1}$ and ε to $10^{-3} m$. The subscript s indicates that the differential operator is considered along the surface Γ_s.

2.1.3. On the interface

The continuity of normal velocity at the interface leads to the relation:

$$\frac{\partial \eta_{tot}}{\partial t} + U \nabla_s \Phi \cdot \nabla_s \eta_{tot} = \frac{\partial \Phi}{\partial \nu} \quad \text{in} \quad \Gamma_s \ \times]0, T[\,, \tag{4}$$

taking account of the rotation of the normal to the surface (cf. [3]).

2.2. Linearization of the governing equations

2.2.1. Steady state

We introduce $(\rho_0, \varphi_0, \eta_0)$ the solution to the Neumann problems:

$$\begin{cases} -\Delta\varphi_0 = 0, \quad \text{in } \Omega \text{ and } \displaystyle\int_{\Gamma_s} \varphi_0 = 0, \\ \dfrac{\partial\varphi_0}{\partial\nu} = 0, \quad \text{in } \Gamma_0 \cup \Gamma_b \cup \Gamma_s, \\ \dfrac{\partial\varphi_0}{\partial\nu} = (e_1 \cdot \nu) \quad \text{in } \Gamma_1 \cup \Gamma_2, \end{cases} \tag{5}$$

and

$$\begin{cases} -\dfrac{\rho_0}{2} U^2 \left\|\nabla_s\varphi_0\right\|^2 + \sigma\Delta_s\eta_0 - \rho_0 g\eta_0 = 0 \quad \text{in} \quad \Gamma_s, \\ \dfrac{\partial\eta_0}{\partial\nu_s} = 0 \quad \text{in} \quad \partial\Gamma_s \end{cases} \tag{6}$$

with $\rho_0 = 10^3 kg.m^{-3}$ and $g = 9.8 m.s^{-2}$. The solution corresponds to a steady quasi uniform horizontal flow with a digging effect due to the term $-\rho_0 U^2 \left\|\nabla_s\varphi_0\right\|^2/2$ (see Figure 2).

2.2.2. Transient state

We study the evolution of a small disturbance around the steady state $(\rho_0, \varphi_0, \eta_0)$. The unsteady waves in the fluid are represented by the perturbation functions ρ, φ, η of $x(x_1, x_2)$ and t. The problem is formulated with them wherein $\rho_{tot}(x,t) = \rho_0(x) + \rho(x,t), \Phi(x,t) = U\varphi_0(x) + \varphi(x,t), \eta_{tot}(x,t) = \eta_0(x) + \eta(x,t)$. The solution is split into a steady state component and a transient one. The domain Ω is then cropped by Γ_0, Γ_b, $\Gamma_s = \eta_0$, Γ_{1equi} and Γ_{2equi}. The new lateral boundaries Γ_{1equi} and Γ_{2equi} correspond to equipotential lines of φ_0 passing respectively through left upper domain corner and right upper corner of Ω. The artificial boundaries are chosen far enough from rigid body to consider that steady state flow is uniform in this area and so the corners of the new domain are right-angled. The disturbance is so small that it is then reasonable to neglect the non-linear terms in the governing equations. Convective derivatives with flow velocity $U\nabla_s\varphi_0$ are used to derive linearized equations for the surface fluid. Hence (ρ, φ, η) are assured to satisfy the linearized enhanced Neumann-Kelvin's model with capillarity:

- the linearized continuity equation,

$$\frac{\partial\rho}{\partial t} + U\nabla\rho \cdot \nabla\varphi_0 + \rho_0\Delta\varphi = 0 \quad \text{in} \quad \Omega \times]0, T[\,. \tag{7}$$

- the linearized momentum equation for the inner fluid,

$$\frac{\partial^2\varphi}{\partial t^2} + 2U\nabla\varphi_0 \cdot \nabla\left(\frac{\partial\varphi}{\partial t}\right) + U^2\nabla\varphi_0 \cdot \nabla(\nabla\varphi_0.\nabla\varphi) - c_f^2\Delta\varphi = 0 \quad \text{in} \quad \Omega \times]0, T[\,. \tag{8}$$

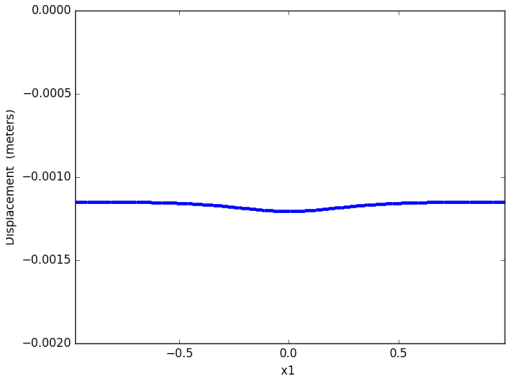

Figure 2: Surface vertical displacement η_0 vs x_1 coordinate with 'digging' effect.

- the linearized momentum equation for the surface fluid,

$$2\varepsilon\rho_0\left(\frac{\partial^2\eta}{\partial t^2} + 2U\nabla_s\varphi_0\cdot\nabla_s\frac{\partial\eta}{\partial t} + U^2\nabla_s\varphi_0\cdot\nabla_s\left(\nabla_s\varphi_0\cdot\nabla_s\eta\right)\right)$$
$$= \sigma\Delta_s\eta - \rho_0 g\eta - \rho_0\frac{\partial\varphi}{\partial t} - \rho_0 U\nabla_s\varphi_0\cdot\nabla_s\varphi \quad \text{in} \quad \Gamma_s\times]0,T[\,. \tag{9}$$

where $\cdot$ denotes the scalar product. Since the domain of study was reshaped the terms $\nabla_s\eta_0$ and $\Delta_s\eta_0$ are set to zero on Γ_s and the continuity of normal velocity at the interface becomes:

$$\frac{\partial\varphi}{\partial\nu} = \frac{\partial\eta}{\partial t} + U\nabla_s\varphi_0\cdot\nabla_s\eta \quad \text{in} \quad \Gamma_s\times]0,T[\,. \tag{10}$$

The non-penetrability condition leads to homogeneous Neumann boundary condition for φ:

$$\frac{\partial\varphi}{\partial\nu} = 0 \quad \text{in} \quad \Gamma_0\cup\Gamma_b\times]0,T[\,. \tag{11}$$

To generate the disturbance of steady state on the surface or in the inner fluid, initial conditions are set by prescribing $\varphi(x,0)$ and $\dfrac{\partial\varphi}{\partial t}(x,0)$ in Ω and $\eta(x,0)$ and $\dfrac{\partial\eta}{\partial t}(x,0)$ in Γ_s.

2.3. Lateral artificial boundary conditions

Finding appropriate artificial boundary conditions able to handle unbounded problems has been an important subject of ongoing research (cf. [5]). Absorbing Boundary Conditions (cf. [4], [6]) or Perfectly Match Layer techniques (cf. [1]) result in our case in multiplying the number of equations to solve and then in increasing the difficulty of the problem. Non-reflecting boundary condition imposed in the following on inner fluid lateral edges is :

$$\frac{\partial \varphi}{\partial t} + \left(U \frac{\partial \varphi_0}{\partial \nu} + c_f \right) \frac{\partial \varphi}{\partial \nu} = 0 \quad \text{in} \quad \Gamma_{1equi} \cup \Gamma_{2equi} \times]0, T[\tag{12}$$

where c_f denotes the speed of sound in the fluid, $c_f = 10^3 m.s^{-1}$. On the surface bounds $\partial\Gamma_s$, the first non-reflecting conditions used are:

$$\frac{\partial \eta}{\partial t} + (U \pm c_r) \frac{\partial \eta}{\partial x_1} = 0 \quad \text{on} \quad x_1 = \pm L \quad \forall t \in]0, T[\tag{13}$$

where c_r denotes the riddle velocity. They are consistent with the natural one dimensional non-reflecting conditions for a propagating wave at velocity c_r in an uniform flow of velocity U. These boundary conditions are successfully applied to modelize the inner fluid (lower layer) wave propagation and the corresponding surface movement (see Figure 4). But the time of simulation required for this case is too short to notice any inaccuracy in the non-reflecting boundary condition for η because of the important difference between the wave velocities in each medium. Therefore propagating phenomenon in each fluid layer can barely be observed with the same time scale. To properly simulate the wave propagation in inner fluid the value of time step chosen is $\Delta t_v = 10^{-5} s$ (see Figure 4) while for surface wave propagation is $\Delta t_s = 10^{-2} s$ (see Figure 3). In addition, singularities in η occur in surface propagating case due to inappropriate reflecting boundary conditions on $\partial\Gamma_s$ (see Figure 3). In fact, singularities appeared on the intersections between the articifial boundary and the interface when standard non-reflecting boundary conditions are imposed. To focus our attention on this issue, we only consider in the remainder of this work, the case where wave propagation is mainly located in surface layer. For the sake of readability only numerical results on normalized η are given in following figures.

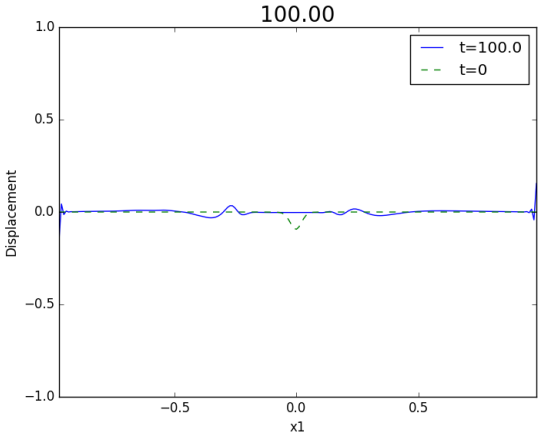

Figure 3: Disturbance η of the surface Γ_s at time $t = 100\Delta t_s$ vs x_1 coordinate. Initial disturbance is located on the surface Γ_s and NRBC used is (13).

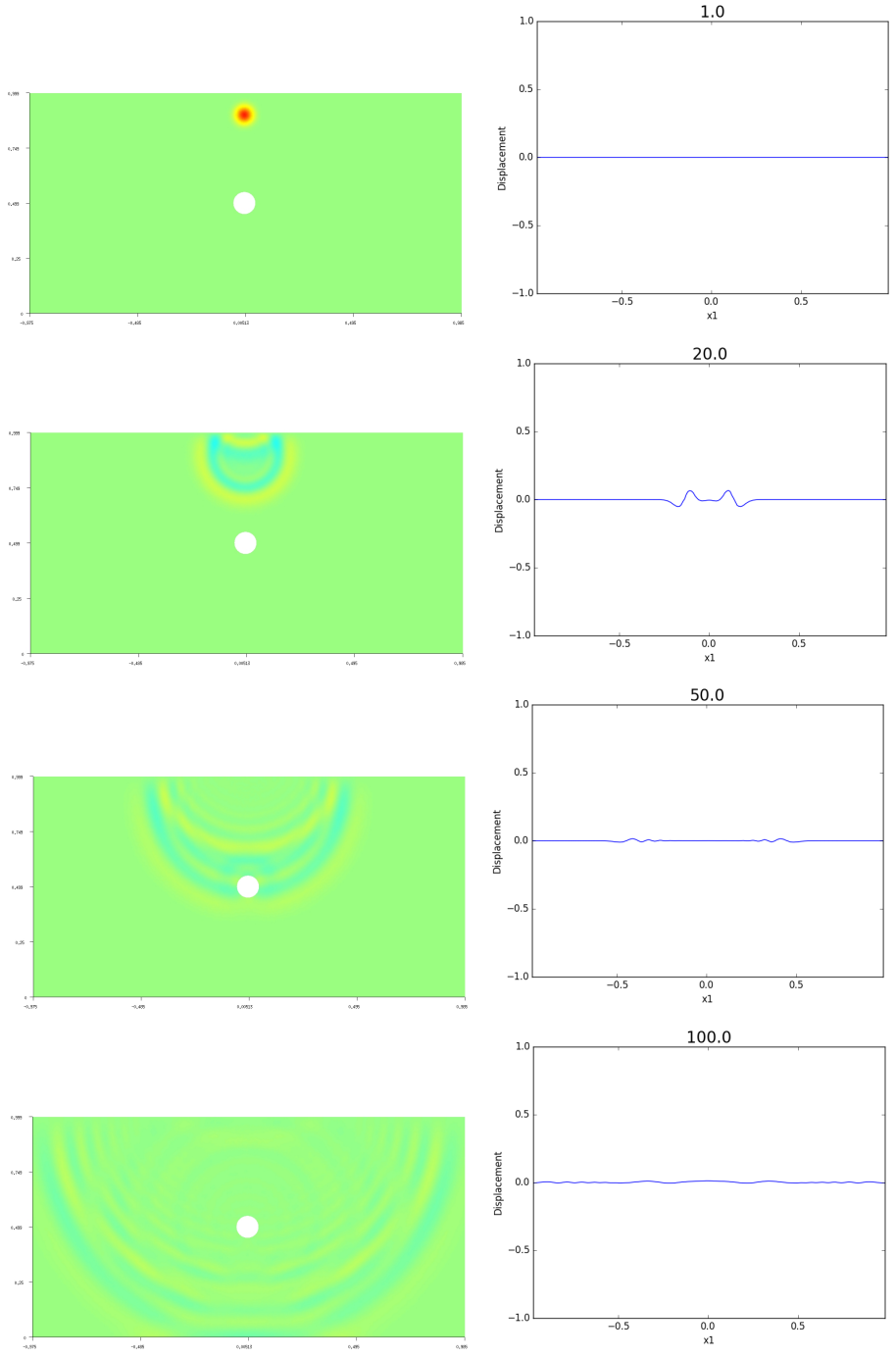

Figure 4: Propagation of disturbance φ in Ω (left column) and matching normal surface displacement η (right column) on Γ_s vs x_1 coordinate at times: $t = \Delta t_v$, $t = 20\Delta t_v$, $t = 50\Delta t_v$, $t = 100\Delta t_v$. Initial disturbance is located in the inner fluid and NRBC used is (13).

To design a new non-reflecting boundary conditions, we express the different terms in the equations (9),(10),(12) on the bounds of the surface $\partial\Gamma_s$. After eliminating the partial derivatives of φ, the small disturbances φ and η must satisfy:

$$Z^{\pm}\frac{\partial\eta(\pm L,t)}{\partial t}+A^{\pm}\frac{\partial\eta(\pm L,t)}{\partial x_1}+B^{\pm}\int_0^t\eta(\pm L,s)ds+C^{\pm}\varphi(\pm L,t)=0\quad\forall t\in\,]0,T[\tag{14}$$

with

$$Z^{\pm}=1+\frac{U\left(U\pm c_f\right)}{(c_r^2-U^2)},A^{\pm}=2U\pm c_f+\frac{2U^2\left(U\pm c_f\right)}{(c_r^2-U^2)},B^{\pm}=\frac{gU\left(U\pm c_f\right)}{2\varepsilon\,(c_r^2-U^2)},C^{\pm}=\frac{\pm Uc_f}{2\varepsilon\,(c_r^2-U^2)}.$$

The symbol $^-$ denotes that condition is on the left boundary of Γ_s and $^+$ on the right one.

§3. Numerical treatment and results

3.1. Variational formulation of the problem

Multiplying (8) by $\psi\in H^1(\Omega)$ and (9) by $v\in H^1(\Gamma_s)$ respectively together with Green's formula and (14) application lead to the regularized variational formulation for the coupled problem (cf. [2]):

Find functions $(\varphi,\eta)\in H^1(\Omega)\times H^1(\Gamma_s)$ such that $\forall(\psi,v)\in H^1(\Omega)\times H^1(\Gamma_s)$,

$$\begin{aligned}
&\int_\Omega\ddot{\varphi}\psi dx+U\int_\Omega\nabla\varphi_0\cdot(\nabla\dot{\varphi}\psi-\dot{\varphi}\nabla\psi)\,dx+c_f\int_\Gamma\dot{\varphi}\psi dx+c_f^2\int_\Omega\nabla\varphi\cdot\nabla\psi dx\\
&-U^2c_f^2\int_\Omega(\nabla\varphi_0\cdot\nabla\varphi)\,(\nabla\varphi_0.\nabla\psi)dx-c_f^2\int_{\Gamma_s}\dot{\eta}\psi dx-Uc_f^2\int_{\Gamma_s}\nabla_s\varphi_0\cdot\nabla_s\eta\,\psi dx=0,\\
&2\varepsilon{c_f}^2\int_{\Gamma_s}\left(\ddot{\eta}v+U\nabla_s\varphi_0\,(\nabla_s\dot{\eta}v-\dot{\eta}\nabla_s v)-U^2(\nabla_s\varphi_0\cdot\nabla_s\eta)(\nabla_s\varphi_0\cdot\nabla_s v)\right)d\sigma\\
&-2\varepsilon c{f^2}U\left(U\int_{\Gamma_s}v\Delta_s\varphi_0\,(\nabla_s\varphi_0\cdot\nabla_s\eta)d\sigma+\int_{\Gamma_s}v\Delta_s\varphi_0\dot{\eta}d\sigma\right)+\frac{c_f^2}{\rho_0}\int_{\Gamma_s}\sigma\nabla_s\eta.\nabla_s v+\rho_0\eta g v\,d\sigma\\
&+c_f^2\int_{\Gamma_s}\dot{\varphi}vd\sigma-\alpha c_f^2U\int_{\Gamma_s}\nabla_s\varphi_0\cdot\nabla_s v\,\varphi d\sigma-\alpha c_f^2U\int v\Delta_s\varphi_0\varphi d\sigma\\
&+(1-\alpha)\,c_f^2U\int_{\Gamma_s}v\nabla_s\varphi_0\cdot\nabla_s\varphi d\sigma+\left[\left(E^{\pm}\dot{\eta}+F^{\pm}\int_0^t\eta\,ds\right)v\right]_{-L}^{L}=0,
\end{aligned} \tag{15}$$

where $E^{\pm}$ and $F^{\pm}$ are functions of $Z^{\pm},A^{\pm},B^{\pm},C^{\pm},c_r,U,g,\varepsilon$ and α is introduced to eliminate $\varphi(L,t)$ and hence improve the regularity of the problem. The term $\varphi(-L,t)$ can be set to zero since φ is determined up to an additive constante.'Over dot' notations are used to denote time partial derivatives.

3.2. Numerical approach and results

The physical field approximation is performed by finite element method and time field approximation by centered finite difference scheme. Meshes are generated by GMSH and FEM

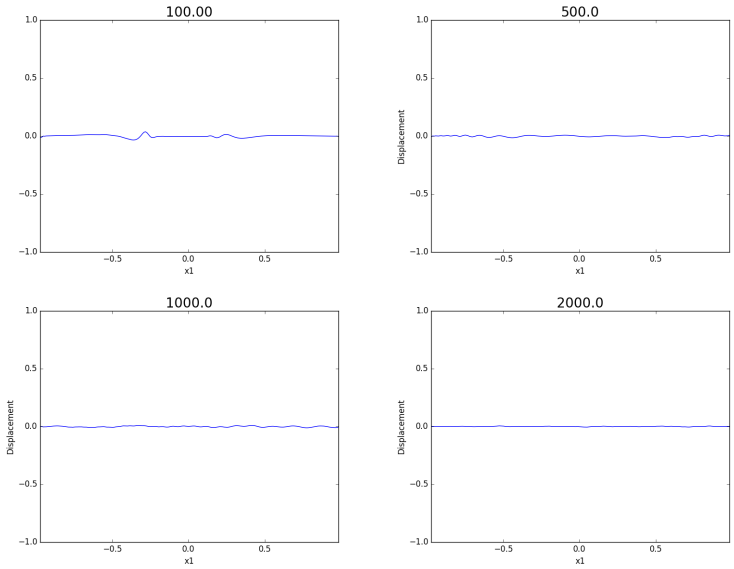

Figure 5: Disturbance η of the surface Γ_s vs x_1 at : $t = 100\Delta t_s,\ t = 500\Delta t_s,\ t = 1000\Delta t_s,\ t = 2000\Delta t_s$. Initial disturbance is located on the surface Γ_s and NRBC used is (14).

calculations are carried out with python module of GETFEM. Only the vertical displacement of the surface is shown since the wave propagation profile is not significant at the time scale concerned. Singularities are no longer present on $\partial\Gamma_s$ and waves can get out of computational domain without generating spurious significant reflections (see Figure 5 and 6) .

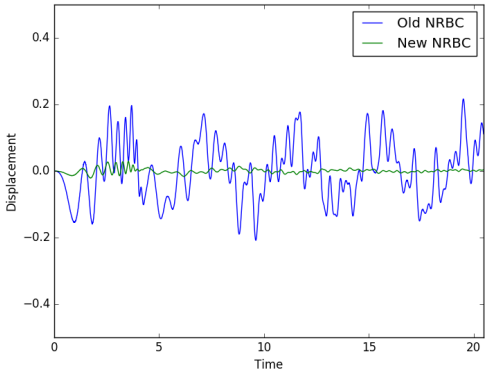

Figure 6: Comparisons of the results for $\eta(-L, t)$ obtained by NRBC (13) and (14) over simulation time $2000\Delta t_s$. Similar results are found for $\eta(L, t)$.

3.3. Conclusion

The modelling of the wake of a solid body in the water leads to deal with a wave propagation problem with complex difficulties. To apply standard methods of resolution intended for bounded domains, artificial boundaries are introduced and appropriate local non-reflecting boundary conditions are devised. They involve neither a big additionnal amount of calculation nor any singularities. Nevertheless to address a more comprehensive case, further investigations need to be done which will be the subjects of future works.

Acknowledgements

I would like to thank Professor Philippe Destuynder for fruitfull discussions.

References

[1] Berenger, J.-P. A perfectly matched layer for the absorption of electromagnetic waves. *Journal of computational physics 114*, 2 (1994), 185–200.

[2] Bissengue, D., and Wilk, O. Conditions aux limites transparentes et modélisation des vagues de surface dans un écoulement. Master's thesis, EICNAM, 2012.

[3] Destuynder, P., and Fabre, C. A discussion on neumann–kelvin's model for progressive water waves. *Applicable Analysis 90*, 12 (2011), 1851–1876.

[4] Engquist, B., and Majda, A. Absorbing boundary conditions for numerical simulation of waves. *Proceedings of the National Academy of Sciences 74*, 5 (1977), 1765–1766.

[5] Givoli, D. *Numerical methods for problems in infinite domains*, vol. 33. Elsevier, 2013.

[6] Halpern, L. Absorbing boundary conditions for the discretization schemes of the one-dimensional wave equation. *Mathematics of Computation 38*, 158 (1982), 415–429.

[7] Lighthill, J. *Waves in fluids*. Cambridge university press, 2001.

[8] Lin, P. A fixed-grid model for simulation of a moving body in free surface flows. *Computers & fluids 36*, 3 (2007), 549–561.

[9] Miles, J. W. On the generation of surface waves by shear flows. *Journal of Fluid Mechanics 3*, 02 (1957), 185–204.

[10] Monaghan, J. J. Simulating free surface flows with sph. *Journal of computational physics 110*, 2 (1994), 399–406.

[11] Piperno, S., Farhat, C., and Larrouturou, B. Partitioned procedures for the transient solution of coupled aroelastic problems, part 1. *Computer methods in applied mechanics and engineering 124*, 1-2 (1995), 79–112.

[12] Stocker, J. Water waves. *Pure and Applied Mathematics 9* (1957), 291–314.

J.M. Orellana
M2N, Departement of mathematics, EPN 6
Conservatoire des Arts et Métiers
292, rue Saint Martin 75141 PARIS Cedex 03
jose.orellana@cnam.fr